Using musculoskeletal models to estimate the effects of exoskeletons on spine loads during dynamic lifting tasks: differences between OpenSim and the AnyBody Modeling System

Mohamad Behjati Ashtiani[1], Mohammadhossein Akhavanfar[2], Lingyu Li[1], Sunwook Kim[1], Maury A. Nussbaum[1]

[1]Department of Industrial and Systems Engineering, Virginia Tech, Blacksburg, VA, USA

[2]School of Human Kinetics, Faculty of Health Sciences, University of Ottawa, Ottawa, Ontario, K1N 6N5, Canada

Mohamad Behjati Ashtiani, Msc. (mohamadbehjati@vt.edu)

Mohammadhossein Akhavanfar, Ph.D. (makha037@uottawa.ca)

Lingyu Li, BSc. (lingyu99@vt.edu)

Sunwook Kim, Ph.D. (sunwook@vt.edu)

***Corresponding Author:**

Maury A Nussbaum, PhD, Virginia Tech

Blacksburg, Virginia, United States.

Email: nussbaum@vt.edu

Phone: (540) 231-6053

Word count (from “Introduction” through “conclusion”): **3805,** Word count (abstract): **229**

Abstract

Occupational back-support exoskeletons (BSEs) can reduce physical demands during lifting by providing assistive torques, but their effects on spine loading are poorly understood. In this study, we used two common musculoskeletal models developed in OpenSim and the AnyBody Modeling System to estimate intervertebral joint forces (IJF) during asymmetric and symmetric lifting tasks with and without BSEs. Data from an earlier study were used, involving 18 participants who performed repetitive lowering/lifting in three task conditions and with three different BSEs (along with a control condition using no BSE). We simulated the tasks with both models and estimated axial compression and anteroposterior shear forces at the L4/L5 joint and derived peak values (95th percentile) as outcome measures. OpenSim estimated significantly larger axial compression and anteroposterior shear forces than AMS. Both models estimated reductions in spine loading when using either of the BSEs, though OpenSim estimated greater reductions than AMS. Strong positive, linear relationships (r >0.95) between the two model estimates were found for axial compression, while much weaker and even negative relationships were observed for shear forces, especially under asymmetric conditions. The differences in model estimates were likely due to variations in model assumptions and passive tissue representations. Future research should explore more detailed human-exoskeleton interaction models, evaluate the impact of modeling assumptions on IJF estimates, and assess the agreement of these findings with *in vivo* measurements such as electromyography.

Keywords:

Back-Support Exoskeletons, Musculoskeletal Modeling, AnyBody Modeling System, OpenSim, Spine

Original Article

Using musculoskeletal models to estimate the effects of exoskeletons on spine loads during dynamic lifting tasks: differences between OpenSim and the AnyBody Modeling System

Mohamad Behjati Ashtiani[1], Mohammadhossein Akhavanfar[2], Lingyu Li[1], Sunwook Kim[1], Maury A Nussbaum[1]

[1]Department of Industrial and Systems Engineering, Virginia Tech, Blacksburg, VA, USA

[2]School of Human Kinetics, Faculty of Health Sciences, University of Ottawa, Ottawa, Ontario, K1N 6N5, Canada

Word count (from “Introduction” through “conclusion”): **3805**

***Corresponding Author:**

Maury A Nussbaum, PhD, Virginia Tech

Blacksburg, Virginia, United States.

Email: nussbaum@vt.edu

Phone: (540) 231-6053

Abstract

Occupational back-support exoskeletons (BSEs) can reduce physical demands during lifting by providing assistive torques, but their effects on spine loading are poorly understood. In this study, we used two common musculoskeletal models developed in OpenSim and the AnyBody Modeling System to estimate intervertebral joint forces (IJF) during asymmetric and symmetric lifting tasks with and without BSEs. Data from an earlier study were used, involving 18 participants who performed repetitive lowering/lifting in three task conditions and with three different BSEs (along with a control condition using no BSE). We simulated the tasks with both models and estimated axial compression and anteroposterior shear forces at the L4/L5 joint and derived peak values (95^{th} percentile) as outcome measures. OpenSim estimated significantly larger axial compression and anteroposterior shear forces than AMS. Both models estimated reductions in spine loading when using either of the BSEs, though OpenSim estimated greater reductions than AMS. Strong positive, linear relationships (r >0.95) between the two model estimates were found for axial compression, while much weaker and even negative relationships were observed for shear forces, especially under asymmetric conditions. The differences in model estimates were likely due to variations in model assumptions and passive tissue representations. Future research should explore more detailed human-exoskeleton interaction models, evaluate the impact of modeling assumptions on IJF estimates, and assess the agreement of these findings with *in vivo* measurements such as electromyography.

Keywords:

Back-Support Exoskeletons, Musculoskeletal Modeling, AnyBody Modeling System, OpenSim, Spine

1. Introduction

Occupational back-support exoskeletons (BSEs) have emerged as an ergonomic intervention that can reduce physical demands on the back during work tasks and thereby potentially reduce the risk of work-related musculoskeletal disorders (de Looze et al., 2016; Kazerooni, 2008; Lee et al., 2012). In particular, BSEs can reduce muscle activity, perceived exertion, and energy expenditure during various manual tasks, including symmetric and asymmetric lifting and prolonged trunk bending (Ali et al., 2021; Kermavnar et al., 2021). The beneficial (and undesirable) effects of BSE use can also depend on various factors including the performed task, BSE design, and individual characteristics such as biological sex (e.g., Alemi et al., 2020; Bosch et al., 2016; Lamers et al., 2017; Madinei et al., 2020). Yet, it remains generally unclear whether BSEs can effectively reduce spine loading, although such loading is a common direct indicator of low back disorder risk (Waters et al., 1993). This uncertainty arises from the wearable nature of BSEs, which complicates estimating spine loading using detailed musculoskeletal models. For example, it is difficult to use models based on surface electromyography (EMG), due to challenges in electrode placement and signal quality while wearing a BSE. While some researchers have used such models to estimate spine loading (Eskandari et al., 2025; Koopman, Kingma, et al., 2020; Koopman, Näf, et al., 2020), the study protocols were limited to short durations and simple lifting tasks.

Musculoskeletal modeling tools, such as the widely used AnyBody Modeling System™ (AMS; Damsgaard et al., 2006) and OpenSim (Delp et al., 2007), have been a basis to virtually design BSEs while accounting for human-exoskeleton interactions (Chander et al., 2022; Ma et al., 2023). Investigators have also used these tools to estimate the effects of BSEs on wearers, finding that BSE use can significantly reduce physical demands, including estimated joint reaction forces and muscle activations (Banks et al., 2024; Madinei & Nussbaum, 2023; Schmalz et al., 2022; Yan et al., 2024). However, there are no reports, to our knowledge, regarding whether different musculoskeletal modeling tools produce consistent estimates of spine loading in dynamic lifting tasks, especially in the context of BSE use. Potential inconsistencies could arise from variations in simulation packages and the differing assumptions underlying the musculoskeletal models within these tools (Ghezelbash et al., 2020; Kim et al., 2018). We believe that identifying potential inconsistencies will help in using these models to guide BSE design and to evaluate BSE biomechanical effects in diverse applications.

In the current study, we compared spine loads estimated from AMS and OpenSim during symmetric and asymmetric lifting and lowering tasks, when both tasks were done with and without two distinct BSEs. This work represents an initial effort to explore the application of these modeling tools in assessing BSE benefits and limitations. Our objective was not to validate modeling outcomes (e.g., against a "gold standard"), but rather to examine the consistency (or inconsistency) of their outputs across different task conditions. To maintain a practical (user-centered) perspective, we compared current versions of the available musculoskeletal models without harmonizing modeling approaches or detailed specifications. Given existing differences in modeling principles and assumptions, we hypothesized that these tools would estimate *quantitatively different* spine loads during BSE use. Nonetheless, based on previous findings on the effects of BSEs on spine loading, we also hypothesized that both tools would yield *qualitatively similar* estimates of such BSE effects.

2. Materials and methods

2.1 Experimental setup and data pre-processing

Data used here were obtained in a previously reported study (Madinei et al., 2020), the details of which are only summarized here. Eighteen participants (9 females, 9 males) performed trials involving repetitive lowering/lifting in each of nine conditions (3 *Task Conditions* × 3 *Interventions*). The *Task Conditions* were: symmetric lowering/lifting to/from mid-shank height (Ground_Sym) and to/from knee height (Knee_Sym), and asymmetric lowering/lifting to/from knee height at a 90º asymmetry angle (Knee_Asy). The *Intervention* levels included two BSEs (suitX backX™ AC and Laevo™ V2.5) and a control condition (no BSE). Each trial comprised 40 cycles of freestyle lowering/lifting a box (set to 10% of individual body mass) from/to a height-adjustable table set to the participant's waist height at a rate of 10 cycles per minute over a 4-min. duration. Whole-body kinematics were recorded at 60 Hz using an inertial motion capture system (MVN Awinda, Xsens Technologies, Netherlands). Kinematic data were exported as BioVision Hierarchy (BVH) files. Each BVH file includes a static hierarchy of 72 degrees-of-freedom (DOF) stick-figure model and a motion section with pelvis positions and YXZ Euler joint rotations in a right-handed local frame (Y=superior, X=left, Z=anterior). Kinematic data were lowpass filtered using a fourth-order, bidirectional, Butterworth filter with a 5 Hz cut-off frequency (Madinei et al., 2020).

2.2 Musculoskeletal models

We used the generic gait-full-body model from the AnyBody™ Managed Modeling Repository (v3.0.1) in AMS. Earlier work showed that this model generated estimates of L4/L5 spine loads that had a strong positive correlation with *in vivo* measurements during dynamic lifting tasks (Bassani et al., 2017). In OpenSim (v4.5), we used the enhanced, fully articulated thoracolumbar spine (FATLS) full-body generic model that was developed by Akhavanfar et al. (2024). Building on the spine model introduced by Bruno et al. (2015), the enhanced FATLS incorporates passive intervertebral stiffness and was demonstrated to estimate resultant L1/L2 spine loads that had a strong positive correlation with direct measurements of vertebral implant forces during dynamic lifting tasks. Also, the original FATLS vertebral compressive loading estimates, including spine loads from the lumbar and thoracic regions of the model (including at L4/L5), were strongly correlated with intradiscal pressure measurements for a variety of symmetric and asymmetric activities (Bruno et al., 2015). Table A1 (see Supplemental Material) provides additional detailed information on the models we used within AMS and OpenSim.

2.3 Lowering and lifting simulation and modeling

AMS and OpenSim estimate muscle activation levels and forces via processes that include: 1) scaling the generic model to match individual anthropometric dimensions and adjusting muscle moment arms and cross-sectional areas; 2) performing an inverse kinematic analysis to obtain joint kinematics; 3) completing an inverse dynamics analysis to obtain the net forces and moments at all joints; and 4) estimating muscle forces by solving a static optimization problem. OpenSim can also include a residual reduction algorithm before the final step, however we excluded this algorithm since we did not have force plate data. Simulations for each experimental trial were performed separately for each lowering and lifting phase using both AMS and OpenSim. In these simulations, we assumed the box mass to be evenly distributed between the hands and added half of the box mass to the mass of each hand segment (Akhavanfar et al., 2022). In the absence of ground reaction force data, residual forces in AMS and reserve actuators in OpenSim were applied to the pelvis to provide the necessary forces for balancing the models. For each participant and experimental condition, intervertebral joint forces (IJFs) were computed at the L4/L5 level. We focused on this level since earlier studies also compared model estimates at this level vs. *in vivo* measurements for tasks where such data were available (Bassani et al., 2017; Bruno et al., 2015).

Implementing the AnyBody Modeling System (AMS)

Using AMS built-in routines, the Gait-full-body model was first scaled to each participant based on segment lengths derived from the BVH files (Karatsidis et al., 2019). This scaling specifically adjusted body segment geometry, mass, inertial properties, and maximum isometric muscle forces (Rasmussen et al., 2005). In AMS, we used the built-in BVH importer to reconstruct the stick-figure model with the same Euler sequence and local coordinate frames. The importer also generated virtual markers (VMs) corresponding to anatomical landmarks on both the human model and the stick figure. Using the motion data from the BVH file, these VMs on the stick figure were tracked in real time and treated as experimental markers (Karatsidis et al., 2019; Skals et al., 2017). Inverse kinematics was performed by aligning virtual marker locations on human models to corresponding VMs from the built-in stick figure model generated from BVH files, using a kinematic optimization that minimized weighted least-squares differences between the VM positions on the stick figure and human model (Andersen et al., 2009). Muscle forces were computed through static optimization, minimizing the sum-of-squared normalized muscle forces while satisfying constraints on equilibrium and the non-negativity of muscle forces (Damsgaard et al., 2006).

To simulate a BSE, we created a virtual representation following the approach outlined by Madinei and Nussbaum (2023). The virtual BSE consisted of three massless dummy segments—a torso and two leg segments—connected via revolute joints. These segments were constrained to the Gait-full-body model at the hip joint, chest, and thighs, allowing them to follow the trunk and hip movement through corresponding contact frames on the BSE and the human model (Figure 1). Real-time support torques generated by each BSE were determined using the angle between these segments and torque-angle data we obtained from the manufacturers (in contrast to Madinei & Nussbaum, 2023, who used their own experimental measures). From the torque and moment arm (the length of the BSE torso segment), we estimated interaction forces between the torso segment and the chest of the Gait-full-body model. These forces were applied to the thorax at a fixed frame located midway between the incisura jugularis and xiphoid process (Figure 1), similar to Eskandari et al. (2025); the position of this frame remained constant throughout the simulations. Detailed information regarding the constraints applied to the BSE segments relative to the human model is provided in the Supplementary Materials.

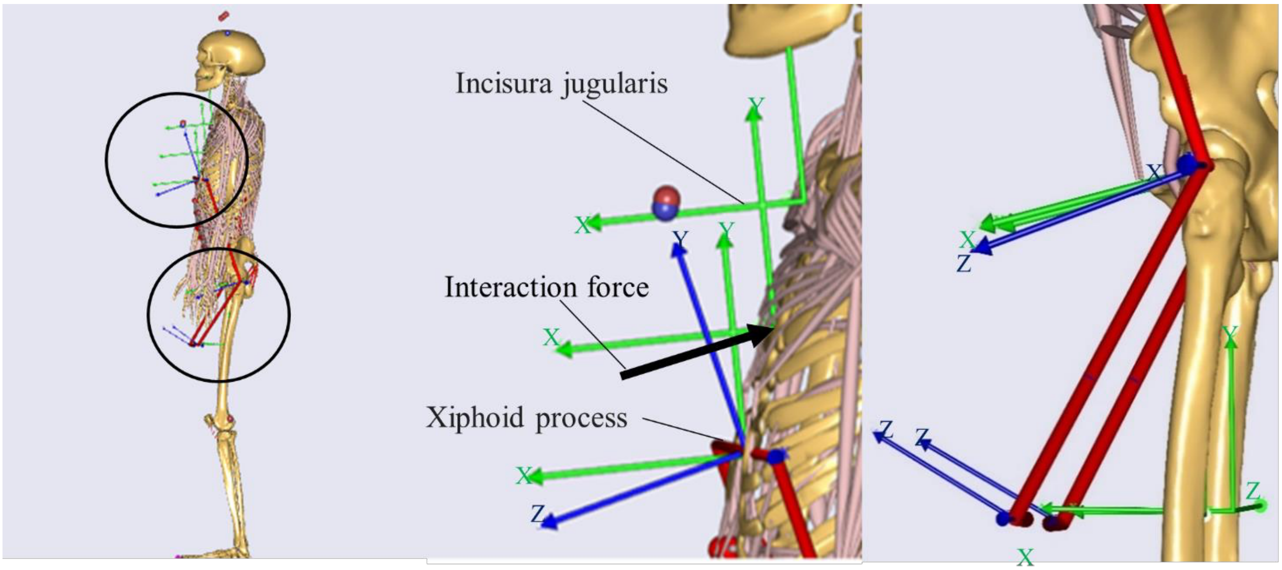

Figure 1. Illustrations of a virtual BSE representation in the AnyBody Modeling System (AMS). The middle and right figures show zoomed-in views of the frames (coordinate systems) for the BSE (blue) and the Gait-full-body model (green) at the torso and leg segment, respectively. The black arrow indicates the interaction force between the BSE and the Gait-full-body model, applied to a fixed frame on the chest — positioned midway between the incisura jugularis and the xiphoid process (green)—and aligned parallel to the Z-axis of the frame located at the midpoint of the top of the torso segment (blue Z-axis).

Implementing OpenSim

The FATLS model was scaled using the Scale Tool (Delp et al., 2007) based on VMs data from a static N-pose (Wechsler et al., 2023) and using anthropometric data to adjust maximum isometric muscle forces (Rasmussen et al., 2005). In OpenSim, a similar approach was used: the stick-figure model was reconstructed using the same rotation sequences defined in the BVH file; VM positions were tracked on the stick-figure model using motion data; and marker data (.trc) for the VMs were extracted following the method described by Wechsler et al. (2023). Inverse kinematics was performed using the Inverse Kinematics Tool, which minimized weighted squared errors between the three-dimensional positions of markers in the FATLS model and the corresponding VMs (Delp et al., 2007). Using the Static Optimization tool, inverse dynamics analysis was performed, followed by static optimization to minimize the sum of squared muscle activations while satisfying constraints on equilibrium and the non-negativity of muscle forces, while accounting for muscle force-length-velocity relationships.

A virtual BSE was added using a similar approach to AMS, comprising three dummy segments (BSE torso and two leg segments) interconnected via custom joints (see Figure 2). Interaction forces were calculated as in AMS and were applied to the thorax. But, the location of force application was defined in the local coordinate system of the BSE torso segment, which was positioned at the midpoint of the top BSE torso segment, parallel to the axis normal to the torso segment (Figure 2) rather than at the fixed frame located on the chest as in AMS. This approach was used so that the application point of the interaction forces corresponded to the contact point of the BSE torso segment at the chest.

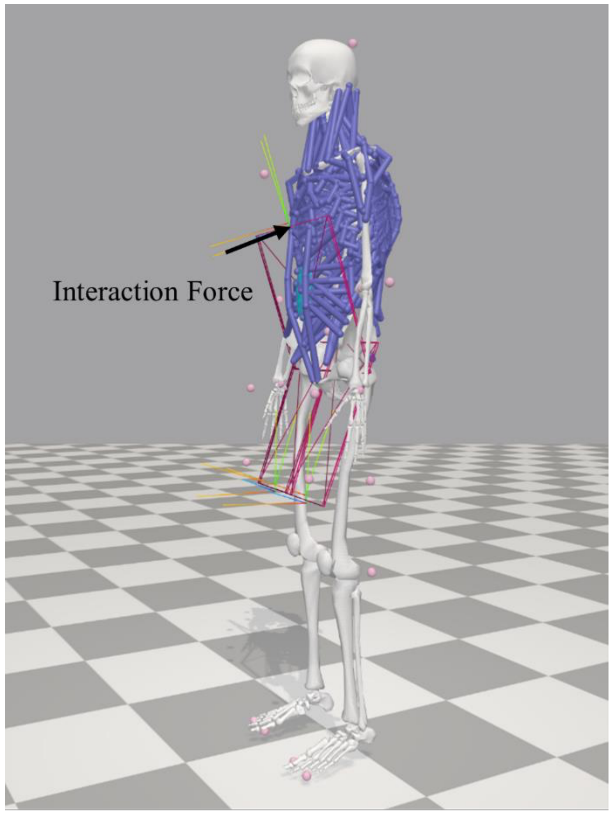

Figure 2. Illustration of the virtual BSE representation in OpenSim. The black arrow represents the interaction force between the BSE and the FATLS model, which is applied to the thorax. Pink balls represent VMs in the human model.

2.4 Data processing and outcome measures

We ran 12,960 simulations, involving 18 participants × 9 trials × 40 cycles × 2 phases (lifting and lowering), in both AMS and OpenSim. Simulations were done using Python libraries—AnyPyTools for AMS (Lund et al., 2019) and the OpenSim API (v4.5). For each simulation, IJFs at the L4/L5 lumbar spine level were extracted and expressed in the L5 local coordinate system, specifically as axial compressive (F_C) and anteroposterior shear (F_{AP}) forces. Mediolateral shear forces were not analyzed since they were consistently of small magnitude (<100 N). We derived peak (95th percentile) values of F_C and F_{AP} as outcome measures within each lift/lower cycle. Peak values were of interest as they are common metrics for ergonomic assessments.

2.5 Statistical Analyses:

Repeated-measures analyses of variance (ANOVAs) were performed using JMP Pro 16 (SAS, Cary, NC) and applying the restricted maximum likelihood method. Four-way ANOVAs were used to assess the effects of *Task Condition*, *Intervention*, *Movement Phase*, and *Model* (i.e., AMS *vs* OpenSim) on peak F_C and F_{AP}, with *Biological Sex* included as a blocking factor. Analyses were limited to three-way interactions to avoid practical difficulties in interpreting higher-order interactions. We also evaluated the linear association between estimates from the two models, by obtaining the Pearson Correlation Coefficient (r) for each lowering/lifting cycle. We then used three-way ANOVAs to examine the effects of *Task Condition*, *Intervention*, and *Movement Phase* on the coefficients. In both sets of ANOVAs, lowering/lifting cycles were treated as replications, and the presentation orders of *Task Condition* and *Intervention* were included as blocking factors (*n.b.*, no significant order effects were found). Statistical significance was concluded when $p < 0.05$. To meet parametric model assumptions, all outcome measures except r for F_{AP} were log-transformed prior to analysis, with summary results back-transformed for presentation. A distinct transformation (Johnson Sb) was applied to the noted r values since there were negative values. Significant main and interaction effects were explored using *post hoc* paired comparisons (using Tukey's HSD) and simple effects tests, respectively. Given the study aims, the subsequent results presentation emphasizes effects involving *Intervention* and *Model*. Detailed ANOVA results are provided in Tables A2 and A3 in the Supplementary Material.

3. Results

3.1 Overall qualitative comparisons between AMS and OpenSim

Model estimates of F_C had similar overall trends, yet OpenSim generally estimated larger values at the end of a lowering task or at the start of lifting, but lower values mid-task (Figures 3-4). Across the lowering/lifting tasks, F_{AP} forces estimated using OpenSim were consistently larger than those from AMS

(Figures 3-4). Additional ensemble plots are presented in Figures A1–A7 in the Supplementary Materials, providing further comparisons between OpenSim and AMS.

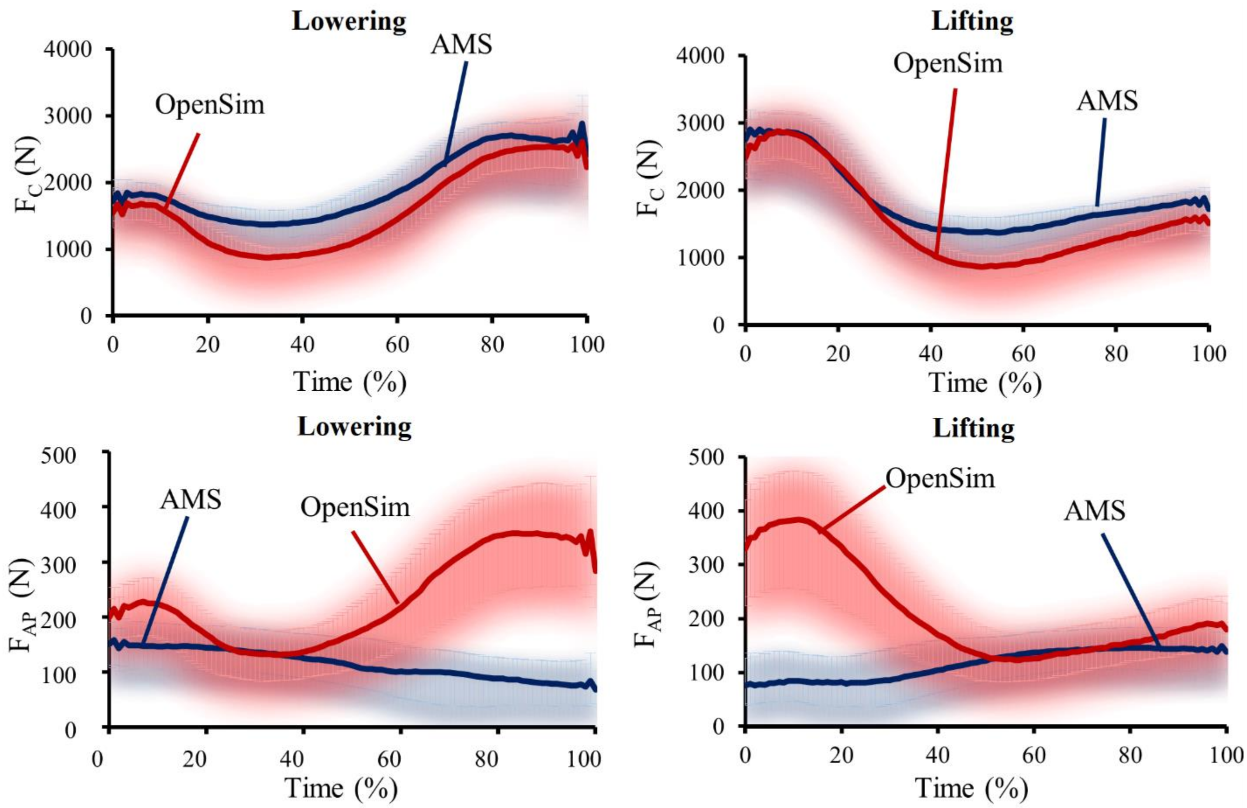

Figure 3. Example ensemble median plots of intervertebral joint forces at the L4/L5 intervertebral joint, comparing results from OpenSim and AnyBody (AMS) for the asymmetric lowering/lifting from/to waist height to/from knee height at a 90° asymmetry angle when using backX. This condition was selected as it represents the “worst” condition, highlighting substantial differences in estimates of F_{AP}. **Top left:** Compression Forces (F_C) during lowering. **Top right:** F_C during lifting. **Bottom left:** Anteroposterior Shear Forces (F_{AP}) during lowering. **Bottom right:** F_{AP} during lifting. Shaded areas represent 25th and 75th percentile values.

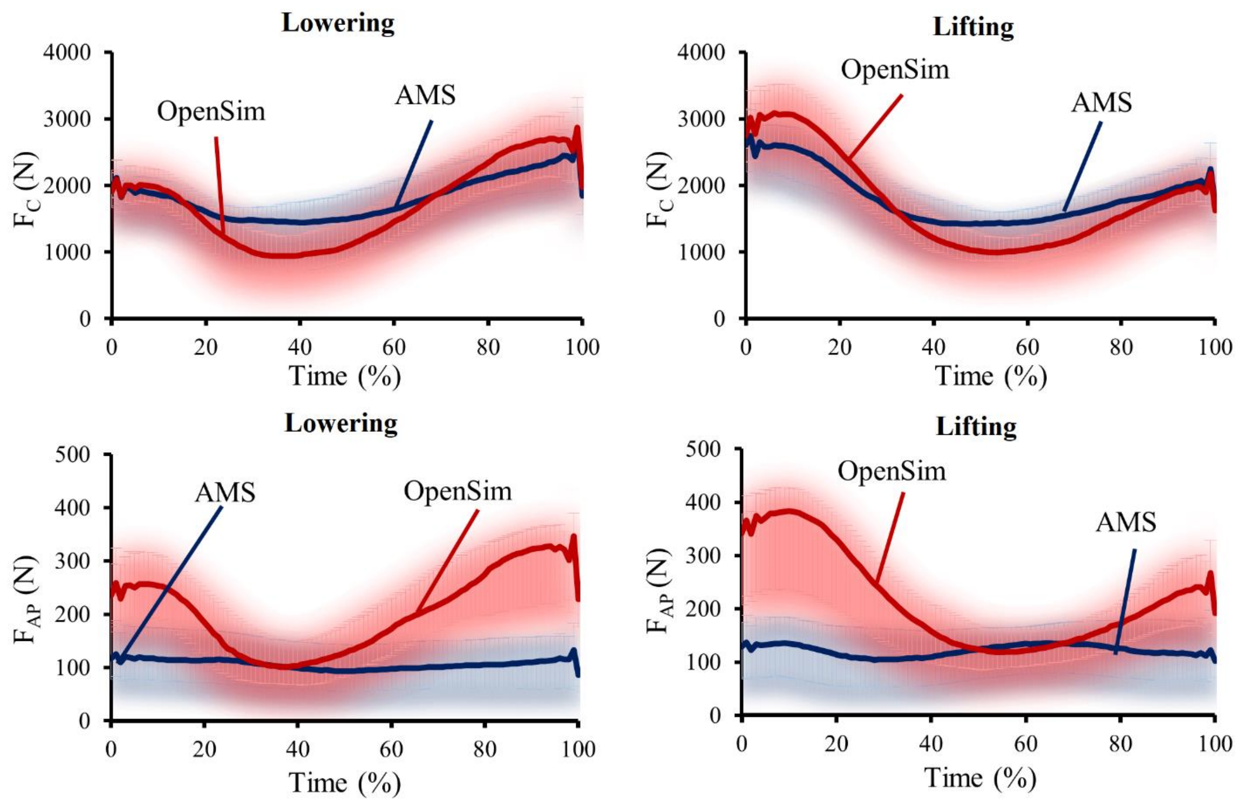

Figure 4. Example ensemble median plots of intervertebral joint forces at the L4/L5 intervertebral joint comparing results from OpenSim and AnyBody (AMS) for the symmetric lowering/lifting from/to waist height to/from knee height when using Laevo. This condition was selected as it represents the “best” condition, with similar trend for estimates of F_{AP}. **Top left:** Compression Forces (F_C) during lowering. **Top right:** F_C during lifting. **Bottom left:** Anteroposterior Shear Forces (F_{AP}) during lowering. **Bottom right:** F_{AP} during lifting. Shaded areas represent the 25th and 75th percentile values.

3.2 Peak compression force (F_C) at L4/L5

The *Task Condition* × *Intervention* × *Model* interaction effect was significant on peak F_C. Simple effects analysis indicated significant *Intervention* × *Model* effects across all *Task Conditions*, as well as significant *Task Condition* × *Model* effects across all *Interventions*. Despite this complexity, there were some consistent outcomes. Specifically, OpenSim estimated significantly larger (9-13%) peak F_C than AMS across all conditions (Figure 5). For each *Task Condition*, both models estimated significantly smaller peak F_C when using a BSE vs. the control condition. Depending on the specific *Task Condition*, such reductions were estimated to be 10-14% in AMS and 14-21% in OpenSim.

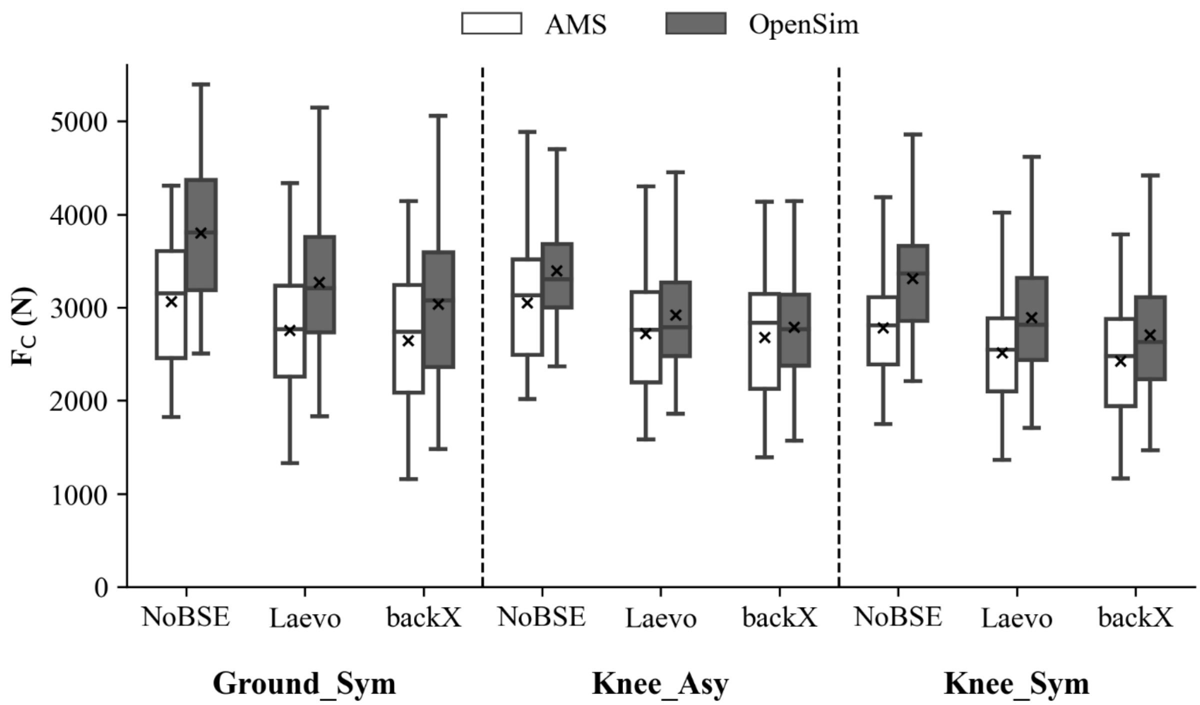

Figure 5. *Task Condition* × *Intervention* × *Model* interaction effect on estimated peak (95th percentile) compressive forces (F_C) at L4/L5 as estimated using the AnyBody Modeling System (AMS) and OpenSim. Task conditions: Ground_Sym refers to symmetric lowering/lifting from/to waist height to/from mid-shank height; Knee_Sym refers to symmetric lowering/lifting from/to waist height to/from knee height; and Knee_Asy refers to asymmetric lowering/lifting from/to waist height to/from knee height at a 90° asymmetry angle.

There was a significant interaction effect of *Intervention* × *Movement Phase* × *Model* on peak F_C. Simple effects analysis indicated a significant interaction effect of *Intervention* × *Model* in both the lowering and lifting phases. Similarly, a significant *Movement Phase* × *Model* interaction effect was observed for all *Intervention* levels. Reductions in peak F_C estimated with BSE use were more pronounced during lowering tasks (Figure 6). BSE use was estimated to decrease peak F_C by 13–16% in AMS and 18–22% in OpenSim during lowering tasks, compared to 9–12% in AMS and 11–17% in OpenSim during lifting tasks.

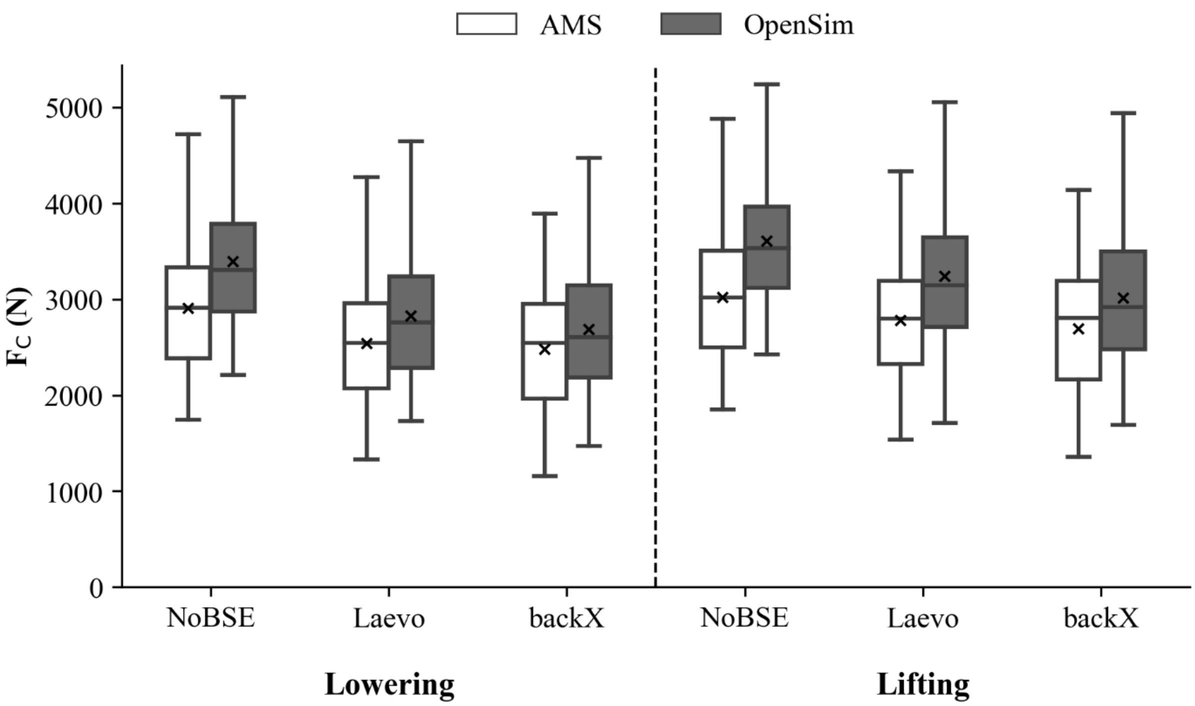

Figure 6. *Intervention* × *Movement Phase* × *Model* interaction effect on peak (95th percentile) compressive forces (F_C) at L4/L5.

3.3 Peak anteroposterior shear forces (F_{AP}) at L4/L5

There was a significant effect of *Intervention* × *Task Condition* × *Model* on peak F_{AP}. Simple effects analysis revealed significant *Intervention* × *Model* and *Task Condition* × *Model* interaction effects for all levels of *Task Condition* and *Intervention*, respectively. Specifically, OpenSim estimated significantly larger peak F_{AP} values than AMS across all conditions (by 119-173%). For all *Task Conditions*, BSE use was estimated to significantly reduce peak F_{AP} values vs. the control condition. Such reductions were by 8-14% in AMS and 14-25% in OpenSim, depending on the specific *Task Condition* (Figure 7).

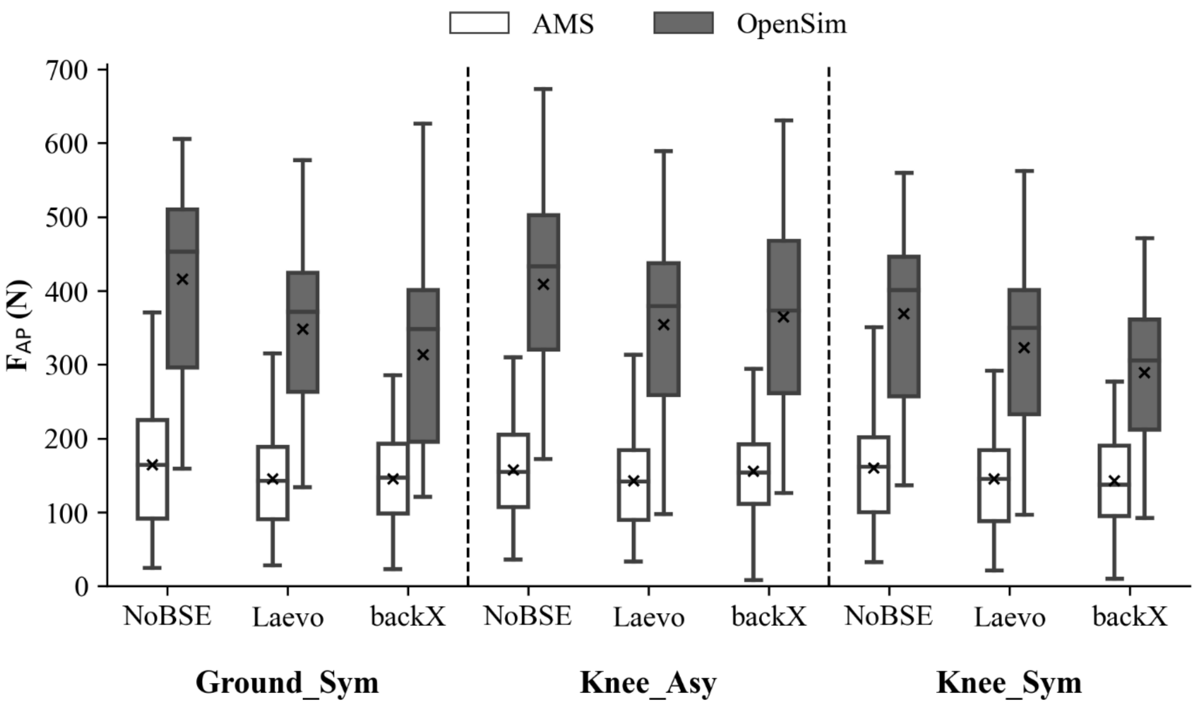

Figure 7. *Task Condition* × *Intervention* × *Model* interaction effect on peak (95th percentile) anteroposterior shear forces (F_{AP}) values at L4/L5. Task conditions: Ground_Sym refers to symmetric lowering/lifting from/to waist height to/from mid-shank height; Knee_Sym refers to symmetric lowering/lifting from/to waist height to/from knee height; and Knee_Asy refers to asymmetric lowering/lifting from/to waist height to/from knee height at a 90° asymmetry angle.

We also found a significant interaction effect of *Intervention* × *Movement Phase* × *Model* on peak F_{AP}. There were significant simple interaction effects of *Movement Phase* × *Model* for all levels of *Intervention*. For both lowering and lifting, there was a significant interaction effect of *Intervention* × *Model.* BSE use was estimated to significantly reduce F_{AP} in AMS during lowering tasks, by 10–11%;

reductions in F_{AP} were more pronounced using OpenSim, ranging from 18–23%. During lifting tasks, the reductions were smaller, being 9–10% in AMS and 12–19% in OpenSim (Figure 8).

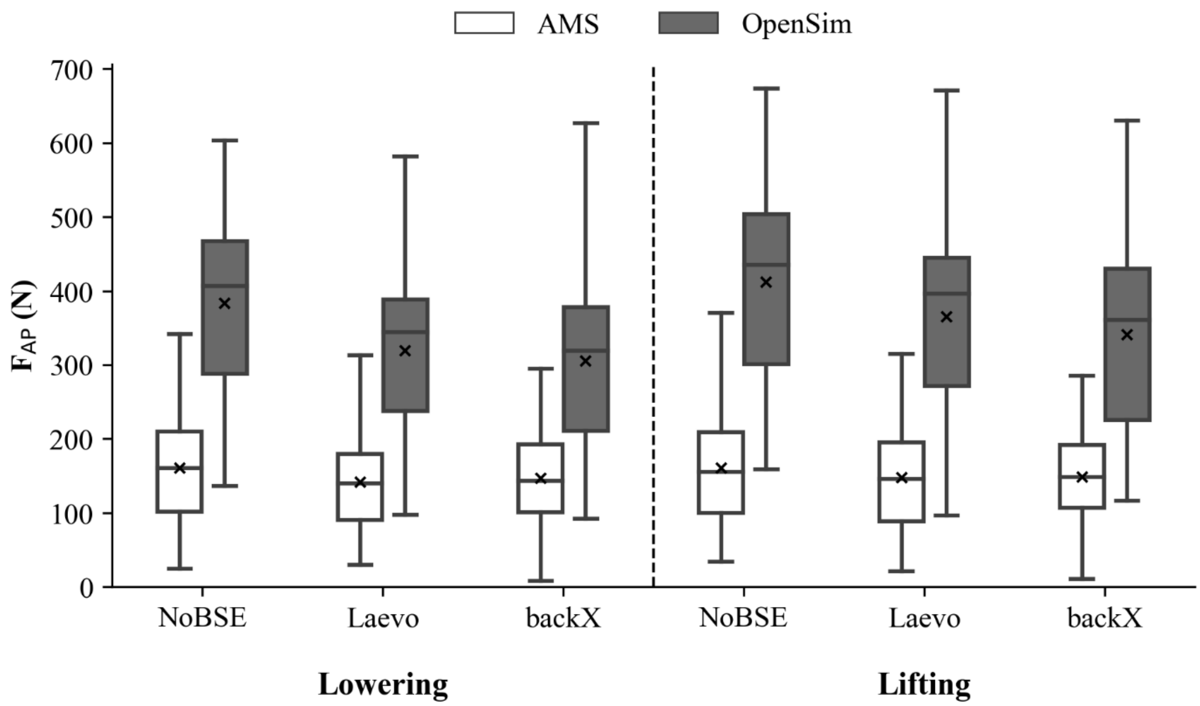

Figure 8. *Intervention* × *Movement Phase* × *Model* interaction effect on peak (95th percentile) anteroposterior shear forces (F_{AP}) values at L4/L5.

3.4 Associations between model estimations (*r*)

For F_C, there were strong, positive, linear relationships between AMS and OpenSim estimations, with the mean r for >0.95 in all *Task Condition* (Figure A8, supplementary materials). In contrast, r values for F_{AP} indicated varied relationships across conditions (Figure 8). Weak positive linear relationships were observed in the Ground_Sym and Knee_Sym conditions, except during the lifting phase when using backX. Of note, moderate-strong *negative* linear relationships were observed in Knee_Asym, regardless of *Intervention* levels.

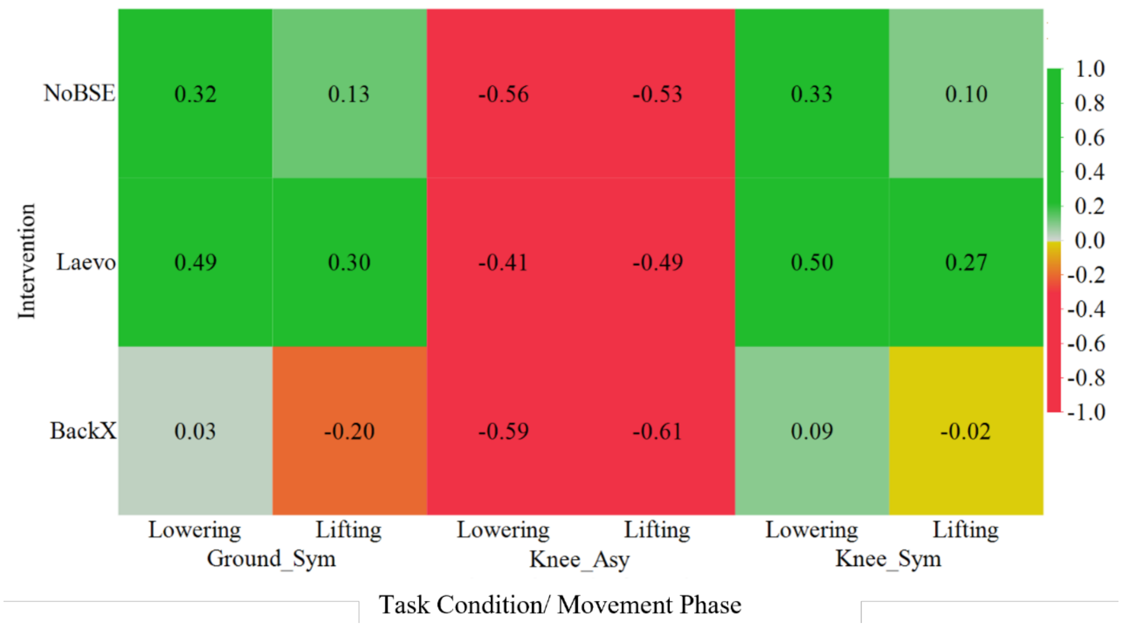

Figure 9. Heatmap of Pearson Correlation Coefficient (*r*) values for F_{AP} times series as estimated by AnyBody (AMS) and OpenSim, across *Task Conditions*, *Interventions*, and *Movement Phases*. Task conditions: Ground_Sym refers to symmetric lowering/lifting from/to waist height to/from mid-shank height; Knee_Sym refers to symmetric lowering/lifting from/to waist height to/from knee height; and Knee_Asy refers to asymmetric lowering/lifting from/to waist height to/from knee height at a 90° asymmetry angle.

4. Discussion

We assessed spine loading estimates obtained from musculoskeletal models using AnyBody and OpenSim during repetitive lowering and lifting tasks, both with and without the use of BSEs. Both modeling tools estimated decreases in spine loading with the use of either of two BSEs compared to the control condition. This finding aligns with previous studies that reported 10–20% reductions in F_C and F_{AP} forces with BSE use (Koopman, Kingma, et al., 2020; Koopman, Näf, et al., 2020; Madinei & Nussbaum, 2023; Schmalz et al., 2022). However, we found that the magnitude of these reductions was larger using OpenSim (Figures 5–8). Associations between F_C time series obtained from the two tools in each experimental condition were generally strong and positive in all experimental conditions (*r* values >0.95). But these associations were both weaker and more variable (ranging from positive to negative) for

F_{AP}. Our findings suggest that, overall, while both modeling tools can assess the effects of BSEs, differences in their outputs should be considered carefully prior to practical decision-making.

We believe there are multiple factors that might account for the larger reductions in IJFs with BSE use when estimated using OpenSim vs. AMS (Figures 5– 8). One such factor is how these tools applied human-exoskeleton interaction forces—derived from BSE supportive torques—and other modeling specifics. In reality, as the user bends forward (or extends), the contact point between the BSE and the chest could move cranially to some extent, shifting the application point of interaction forces on the body further from the lower back. In OpenSim, by defining the interaction force position in the local coordinate system of the BSE torso segment, the position of interaction force could follow the movement of the torso segment on body. However, implementing a similar approach in AMS was not straightforward. Thus, we applied interaction forces in AMS at a fixed location, as in Eskandari et al. (2025). During trunk flexion, the external torque about L4/L5—resulting from the BSE interaction force applied to the human model—may be smaller in AMS than in OpenSim for the same interaction force in extreme postures, potentially contributing to the observed differences in the reduction IJF values.

Despite these differences, F_C time series from AMS and OpenSim had strong, positive associations across all lifting conditions (Figure A8). In contrast, F_{AP} time series showed much weaker associations between ASM and OpenSim, particularly in the Knee-Asy and Ground-Sym conditions (Figures 3, 4, and 9). We suspect that an important contributor to these discrepancies is the difference in how passive intervertebral tissues are represented in the models. The AMS GaitFullBody model includes nonlinear passive elastic elements to account for ligamentous structures and disc stiffness (Chazal et al., 1985; Han et al., 2012). In contrast, the enhanced FATLS model in OpenSim uses bushing elements—a simplified approach that models passive tissue contributions as joint-level passive torques in the spine (Akhavanfar et al., 2024). Other differences in spine-modeling assumptions may also have contributed to divergences in model estimates, including optimization strategies (Wang et al., 2022), muscle architecture (Bruno et al., 2017), spine mechanical modeling (Ghezelbash et al., 2018; Ignasiak et al., 2016), and subject-specific scaling algorithms (Ghezelbash et al., 2016). For example, the OpenSim model includes a fully articulated spine from the thorax to the pelvis, whereas the AMS uses a rigid thorax. A detailed analysis of the underlying sources of differences in the estimated IJFs was beyond our current scope, but we hope to complete such analyses in follow-up work.

Several limitations in the current work were noted earlier by Madinei and Nussbaum (2023), including neglecting the effects of BSE mass and any relative displacements between the BSE and human hip joints, as well as errors related to reconstructing motion data from the inertial motion capture system. Some additional limitations should be acknowledged. First, our virtual BSE representation was simplified by excluding inertial properties and soft materials (e.g., straps and belts). The human-exoskeleton interface was also simplified by using kinematic constraints (Ferrati et al., 2013; Madinei & Nussbaum, 2023; Zhou et al., 2017), rather than using more complex and potentially more realistic approaches such as force-generating elements (Fournier et al., 2018; Tröster et al., 2020) or rigid-body contact force modeling (Chander et al., 2022; Cho et al., 2012). While these methods could offer greater accuracy, they are also quite computationally expensive, particularly for large-scale simulations. Future research should focus on how to best balance model complexity with computational efficiency for BSE (and other exoskeleton) modeling. Second, although there is evidence that estimates from OpenSim and AMS align with *in vivo* data (Alemi et al., 2023; Bassani et al., 2017; Yan et al., 2024), these evaluations have focused primarily on symmetric or simple tasks. The fidelity and applicability of both models to asymmetric tasks or activities involving BSEs remain unclear (e.g., due to simplifications of the human-exoskeleton interface noted above). Our results indicate that either tool can capture the effects of a BSE on spine loading; however, the discrepancies between their outputs highlight the potential need for a more careful evaluation of their accuracy. We thus encourage future comparisons between modeling tools across various exoskeleton types and manual tasks.

In summary, we found that both AMS and OpenSim estimate that BSE use significantly reduced spine loading during symmetric and asymmetric lifting tasks. Both models indicated that BSE use significantly reduces peak F_C and F_{AP}, underscoring the potential of musculoskeletal modeling in assessing BSEs as an ergonomic intervention. However, OpenSim consistently estimated larger overall IJF values and larger reductions in IJFs when using a BSE, particularly for F_{AP}. Strong positive associations were found in F_C estimated between the two models, whereas F_{AP} estimates showed substantially weaker associations, particularly in extreme postures. These discrepancies may have arisen from differences in how the models account for passive structures and force redistribution during lifting motions. Future research should focus on refining human-exoskeleton interaction models, incorporating more realistic representations of passive tissues, and validating findings against *in vivo* data to improve the accuracy and applicability of musculoskeletal simulations for exoskeletons as an ergonomic intervention.

5. Acknowledgment

This study was supported by Grant # 2202862 from the National Science Foundation (NSF). The sponsor was not involved in data analysis, interpretation, or the decision to publish. The current contents are solely the responsibility of the authors and do not necessarily reflect the views of NSF. We thank Advanced Research Computing at Virginia Tech for providing computational resources and technical support that contributed to the results reported in this paper. URL: https://arc.vt.edu/

6. Declaration of generative AI and AI-assisted technologies in the writing process

During the preparation of this work, we used ChatGPT to refine some sentences and improve the clarity of the text. After using this tool/service, we reviewed and edited the content as needed, and we take full responsibility for the content of this publication.

References

Akhavanfar, M., Mir-Orefice, A., Uchida, T. K., & Graham, R. B. (2024). An Enhanced Spine Model Validated for Simulating Dynamic Lifting Tasks in OpenSim. *Annals of Biomedical Engineering*, *52*(2), 259-269. https://doi.org/10.1007/s10439-023-03368-x

Akhavanfar, M., Uchida, T. K., Clouthier, A. L., & Graham, R. B. (2022). Sharing the load: modeling loads in OpenSim to simulate two-handed lifting. *Multibody System Dynamics*, *54*(2), 213-234. https://doi.org/10.1007/s11044-021-09808-7

Alemi, M. M., Banks, J. J., Lynch, A. C., Allaire, B. T., Bouxsein, M. L., & Anderson, D. E. (2023). EMG validation of a subject-specific thoracolumbar spine musculoskeletal model during dynamic activities in older adults. *Annals of Biomedical Engineering*, *51*(10), 2313-2322. https://doi.org/10.1007/s10439-023-03273-3

Alemi, M. M., Madinei, S., Kim, S., Srinivasan, D., & Nussbaum, M. A. (2020). Effects of two passive back-support exoskeletons on muscle activity, energy expenditure, and subjective assessments during repetitive lifting. *Human factors*, *62*(3), 458-474. https://doi.org/10.1177/0018720819897669

Ali, A., Fontanari, V., Schmoelz, W., & Agrawal, S. K. (2021). Systematic review of back-support exoskeletons and soft robotic suits. *Frontiers in bioengineering and biotechnology*, *9*, 765257. https://doi.org/10.3389/fbioe.2021.765257

Andersen, M. S., Damsgaard, M., & Rasmussen, J. (2009). Kinematic analysis of over-determinate biomechanical systems. *Computer methods in biomechanics and biomedical engineering*, *12*(4), 371-384. https://doi.org/10.1080/10255840802459412

Banks, J. J., Quirk, D. A., Chung, J., Cherin, J. M., Walsh, C. J., & Anderson, D. E. (2024). The effect of a soft active back support exosuit on trunk motion and thoracolumbar spine loading during squat and stoop lifts. *Ergonomics*, 1-14. https://doi.org/10.1080/00140139.2024.2320355

Bassani, T., Stucovitz, E., Qian, Z., Briguglio, M., & Galbusera, F. (2017). Validation of the AnyBody full body musculoskeletal model in computing lumbar spine loads at L4L5 level. *Journal of Biomechanics*, *58*, 89-96. https://doi.org/10.1080/10255840802459412

Bosch, T., van Eck, J., Knitel, K., & de Looze, M. (2016). The effects of a passive exoskeleton on muscle activity, discomfort and endurance time in forward bending work. *Applied ergonomics*, *54*, 212-217. https://doi.org/10.1016/j.apergo.2015.12.003

Bruno, A. G., Bouxsein, M. L., & Anderson, D. E. (2015). Development and validation of a musculoskeletal model of the fully articulated thoracolumbar spine and rib cage. *Journal of biomechanical engineering*, *137*(8), 081003. https://doi.org/10.1115/1.4030408

Bruno, A. G., Burkhart, K., Allaire, B., Anderson, D. E., & Bouxsein, M. L. (2017). Spinal loading patterns from biomechanical modeling explain the high incidence of vertebral fractures in the thoracolumbar region. *Journal of Bone and Mineral Research*, *32*(6), 1282-1290. https://doi.org/10.1002/jbmr.3113

Chander, D. S., Böhme, M., Andersen, M. S., Rasmussen, J., Zentner, J., & Cavatorta, M. P. (2022). A comparison of different methods for modelling the physical human-exoskeleton interface. *International journal of human factors modelling and simulation*, *7*(3-4), 204-230. https://doi.org/10.1504/IJHFMS.2022.124310

Chazal, J., Tanguy, A., Bourges, M., Gaurel, G., Escande, G., Guillot, M., & Vanneuville, G. (1985). Biomechanical properties of spinal ligaments and a histological study of the supraspinal ligament in traction. *Journal of Biomechanics*, *18*(3), 167-176. https://doi.org/10.1016/0021-9290(85)90202-7

Cho, K., Kim, Y., Yi, D., Jung, M., & Lee, K. (2012). Analysis and evaluation of a combined human-exoskeleton model under two different constraints condition. *Proceedings of the International Summit on Human Simulation*, *5*, 23-25.

Damsgaard, M., Rasmussen, J., Christensen, S. T., Surma, E., & De Zee, M. (2006). Analysis of musculoskeletal systems in the AnyBody Modeling System. *Simulation Modelling Practice and Theory*, *14*(8), 1100-1111. https://doi.org/10.1016/j.simpat.2006.09.001

de Looze, M. P., Bosch, T., Krause, F., Stadler, K. S., & O'sullivan, L. W. (2016). Exoskeletons for industrial application and their potential effects on physical work load. *Ergonomics*, *59*(5), 671-681. https://doi.org/10.1080/00140139.2015.1081988

Delp, S. L., Anderson, F. C., Arnold, A. S., Loan, P., Habib, A., John, C. T., Guendelman, E., & Thelen, D. G. (2007). OpenSim: open-source software to create and analyze dynamic simulations of movement. *IEEE Transactions on Biomedical Engineering*, *54*(11), 1940-1950. https://doi.org/10.1109/TBME.2007.901024

Eskandari, A. H., Ghezelbash, F., Shirazi-Adl, A., Arjmand, N., & Larivière, C. (2025). Effect of a back-support exoskeleton on internal forces and lumbar spine stability during low load lifting task. *Applied ergonomics*, *123*, 104407. https://doi.org/10.1016/j.apergo.2024.104407

Ferrati, F., Bortoletto, R., & Pagello, E. (2013). Virtual modelling of a real exoskeleton constrained to a human musculoskeletal model. *Biomimetic and Biohybrid Systems: Second International Conference, Living Machines 2013, London, UK, July 29–August 2, 2013. Proceedings 2*, 96-107. https://doi.org/10.1007/978-3-642-39802-5_9

Fournier, B. N., Lemaire, E. D., Smith, A. J., & Doumit, M. (2018). Modeling and simulation of a lower extremity powered exoskeleton. *IEEE transactions on neural systems and rehabilitation engineering*, *26*(8), 1596-1603. https://doi.org/10.1109/TNSRE.2018.2854605

Ghezelbash, F., Eskandari, A., Shirazi-Adl, A., Arjmand, N., El-Ouaaid, Z., & Plamondon, A. (2018). Effects of motion segment simulation and joint positioning on spinal loads in trunk musculoskeletal models. *Journal of Biomechanics*, *70*, 149-156. https://doi.org/10.1016/j.jbiomech.2017.07.014

Ghezelbash, F., Shirazi-Adl, A., Arjmand, N., El-Ouaaid, Z., & Plamondon, A. (2016). Subject-specific biomechanics of trunk: musculoskeletal scaling, internal loads and intradiscal pressure estimation. *Biomechanics and modeling in mechanobiology*, *15*, 1699-1712. https://doi.org/10.1007/s10237-016-0792-3

Ghezelbash, F., Shirazi-Adl, A., Plamondon, A., & Arjmand, N. (2020). Comparison of different lifting analysis tools in estimating lower spinal loads–Evaluation of NIOSH criterion. *Journal of Biomechanics*, *112*, 110024. https://doi.org/10.1016/j.jbiomech.2020.110024

Han, K.-S., Zander, T., Taylor, W. R., & Rohlmann, A. (2012). An enhanced and validated generic thoraco-lumbar spine model for prediction of muscle forces. *Medical engineering & physics*, *34*(6), 709-716. https://doi.org/10.1016/j.medengphy.2011.09.014

Ignasiak, D., Ferguson, S. J., & Arjmand, N. (2016). A rigid thorax assumption affects model loading predictions at the upper but not lower lumbar levels. *Journal of Biomechanics*, *49*(13), 3074-3078. https://doi.org/10.1016/j.jbiomech.2016.07.006

Karatsidis, A., Jung, M., Schepers, H. M., Bellusci, G., de Zee, M., Veltink, P. H., & Andersen, M. S. (2019). Musculoskeletal model-based inverse dynamic analysis under ambulatory conditions using inertial motion capture. *Medical Engineering & Physics*, *65*, 68-77. https://doi.org/10.1016/j.medengphy.2018.12.021

Kazerooni, H. (2008). A review of the exoskeleton and human augmentation technology. *Dynamic Systems and Control Conference*, *43352*, 1539-1547. https://doi.org/10.1115/DSCC2008-2407

Kermavnar, T., de Vries, A. W., de Looze, M. P., & O'Sullivan, L. W. (2021). Effects of industrial back-support exoskeletons on body loading and user experience: An updated systematic review. *Ergonomics*, *64*(6), 685-711. https://doi.org/10.1080/00140139.2020.1870162

Kim, Y., Jung, Y., Choi, W., Lee, K., & Koo, S. (2018). Similarities and differences between musculoskeletal simulations of OpenSim and AnyBody modeling system. *Journal of Mechanical Science and Technology*, *32*, 6037-6044. https://doi.org/10.1007/s12206-018-1154-0

Koopman, A. S., Kingma, I., de Looze, M. P., & van Dieën, J. H. (2020). Effects of a passive back exoskeleton on the mechanical loading of the low-back during symmetric lifting. *Journal of Biomechanics*, *102*, 109486. https://doi.org/10.1016/j.jbiomech.2019.109486

Koopman, A. S., Näf, M., Baltrusch, S. J., Kingma, I., Rodriguez-Guerrero, C., Babič, J., de Looze, M. P., & van Dieën, J. H. (2020). Biomechanical evaluation of a new passive back support exoskeleton. *Journal of Biomechanics*, *105*, 109795. https://doi.org/10.1016/j.jbiomech.2020.109795

Lamers, E. P., Yang, A. J., & Zelik, K. E. (2017). Feasibility of a biomechanically-assistive garment to reduce low back loading during leaning and lifting. *IEEE Transactions on Biomedical Engineering*, *65*(8), 1674-1680. https://doi.org/10.1109/TBME.2017.2761455

Lee, H., Kim, W., Han, J., & Han, C. (2012). The technical trend of the exoskeleton robot system for human power assistance. *International Journal of Precision Engineering and Manufacturing*, *13*, 1491-1497. https://doi.org/10.1007/s12541-012-0197-x

Lund, M. E., Rasmussen, J., & Andersen, M. S. (2019). AnyPyTools: A Python package for reproducible research with the AnyBody Modeling System. *The Journal of Open Source Software*, *4*(33), 1108. https://doi.org/10.21105/joss.01108

Ma, T., Zhang, Y., Choi, S. D., & Xiong, S. (2023). Modelling for design and evaluation of industrial exoskeletons: A systematic review. *Applied ergonomics*, *113*, 104100. https://doi.org/10.1016/j.apergo.2023.104100

Madinei, S., Alemi, M. M., Kim, S., Srinivasan, D., & Nussbaum, M. A. (2020). Biomechanical assessment of two back-support exoskeletons in symmetric and asymmetric repetitive lifting with moderate postural demands. *Applied Ergonomics*, *88*, 103156.

Madinei, S., & Nussbaum, M. A. (2023). Estimating lumbar spine loading when using back-support exoskeletons in lifting tasks. *Journal of Biomechanics*, *147*, 111439. https://doi.org/10.1016/j.jbiomech.2023.111439

Rasmussen, J., de Zee, M., Damsgaard, M., Christensen, S. T., Marek, C., & Siebertz, K. (2005). A general method for scaling musculo-skeletal models. *2005 international symposium on computer simulation in biomechanics*.

Schmalz, T., Colienne, A., Bywater, E., Fritzsche, L., Gärtner, C., Bellmann, M., Reimer, S., & Ernst, M. (2022). A passive back-support exoskeleton for manual materials handling: reduction of low back loading and metabolic effort during repetitive lifting. *IISE transactions on occupational ergonomics and human factors*, *10*(1), 7-20. https://doi.org/10.1080/24725838.2021.2005720

Skals, S., Rasmussen, K. P., Bendtsen, K. M., Yang, J., & Andersen, M. S. (2017). A musculoskeletal model driven by dual Microsoft Kinect Sensor data. *Multibody System Dynamics*, *41*, 297-316. https://doi.org/10.1007/s11044-017-9573-8

Tröster, M., Wagner, D., Müller-Graf, F., Maufroy, C., Schneider, U., & Bauernhansl, T. (2020). Biomechanical model-based development of an active occupational upper-limb exoskeleton to support healthcare workers in the surgery waiting room. *International Journal of Environmental Research and Public Health*, *17*(14), 5140. https://doi.org/10.3390/ijerph17145140

Wang, W., Wang, D., & Li, G. (2022). Towards improving the accuracy of musculoskeletal simulation of dynamic three-dimensional spine rotations with optimizing model and algorithm. *Medical Engineering & Physics*, *110*, 103916. https://doi.org/10.1016/j.medengphy.2022.103916

Waters, T. R., Putz-Anderson, V., Garg, A., & Fine, L. J. (1993). Revised NIOSH equation for the design and evaluation of manual lifting tasks. *Ergonomics*, *36*(7), 749-776. https://doi.org/10.1080/00140139308967940

Wechsler, I., Wolf, A., Fleischmann, S., Waibel, J., Molz, C., Scherb, D., Shanbhag, J., Franz, M., Wartzack, S., & Miehling, J. (2023). Method for using IMU-based experimental motion data in BVH format for musculoskeletal simulations via OpenSim. *Sensors*, *23*(12), 5423. https://doi.org/10.3390/s23125423

Yan, C., Banks, J. J., Allaire, B. T., Quirk, D. A., Chung, J., Walsh, C. J., & Anderson, D. E. (2024). Musculoskeletal models determine the effect of a soft active exosuit on muscle activations and forces during lifting and lowering tasks. *Journal of Biomechanics*, *176*, 112322. https://doi.org/10.1016/j.jbiomech.2024.112322

Zhou, L., Li, Y., & Bai, S. (2017). A human-centered design optimization approach for robotic exoskeletons through biomechanical simulation. *Robotics and Autonomous Systems*, *91*, 337-347. https://doi.org/10.1016/j.robot.2016.12.012